ISSN 1070-3632, Russian Journal of General Chemistry, 2024, Vol. 94, No. 8, pp. 2038–2043. © Pleiades Publishing, Ltd., 2024.

Preparation and Characterization of Pyridin-2-amine Functionalized Thiadiazole-Embedded Polymer Inclusion Membrane and Utilization of Its Heavy Metal Transport Efficiency

M. Cicek[a], S. Cay[a],*, M. S. Engin[b], N. Şener[c], A. E. O. Aldwib[d], and M. Gür[e]

[a] *Department of Environmental Engineering, Faculty of Engineering, Giresun University, Giresun, 28200 Turkey*
[b] *Department of Food Engineering, Faculty of Engineering, Giresun University, Giresun, 28200 Turkey*
[c] *Department of Chemistry, Faculty of Science, Kastamonu University, Kastamonu, 37200 Turkey*
[d] *Institute of Science, Kastamonu University, Kastamonu, 37200 Turkey*
[e] *Department of Forest Industrial Engineering, Faculty of Forestry, Kastamonu University, Kastamonu, 37100 Turkey*
**e-mail: seydahmet.cay@giresun.edu.tr*

Received April 4, 2024; revised July 24, 2024; accepted July 25, 2024

Abstract—3-[5-(Cycloheximino)-4,5-dihydro-1,3,4-thiadiazol-2-yl]pyridine-2-amine was synthesized and used to make a novel pyrazole derivative embedded polymer inclusion membrane (Py@PIM). The surface and structure morphology of Py@PIM was detected using thermogravimetric analysis, FT-IR spectroscopy and scanning electron microscopy. Donnan dialysis system was also used to assess the transport efficacy of Py@PIM towards 5 heavy metals (Co, Cd, Cu, Ni, Pb). The results show that according to the kinetic coefficient, the order is Pb > Ni > Co > Cd > Cu. Similar kinetic order was also observed in multiple cation experiments, in experiments where all cations were mixed in a single cell.

Keywords: thiadiazole, heavy metals, polymer inclusion membrane, surface characterization

DOI: 10.1134/S1070363224080176

INTRODUCTION

The increase in heavy metals observed in accumulation environments as a result of the disruption of natural cycles and as process intermediates or outputs of industrial applications is a dangerous and therefore undesirable situation for humanity. Heavy metal derivatives are harmful to many systems of the human body, such as the excretory system and the nervous system [1, 2]. In short, these metals are essential elements and cause both acute and chronic poisoning above a certain concentration [3]. Therefore, they are metals that need to be recovered and transformed [4].

In addition to this, the studies developed in recent years to reduce water consumption are very important in terms of reuse of water, which is the output of many points of the system, in industrial processes with remediation and feedback. Without adequate treatment, these heavy metals will enter water bodies and cause serious damage to the environment and ecosystems. Moreover, industrial wastewater is seen as an alternative source of water in environmental programs that include water sustainability [5].

Recent studies have focused on solving this problem in a way that is economically cost-effective and relatively easy to implement by studying the physical and chemical properties of heavy metals. The important point here is the selective removal of heavy metals from the environment. While the targeted heavy metals are removed, the lack of reaction to others increases the functionality and importance of the application. The problem is that heavy metals are not biodegradable and therefore tend to accumulate in the environment. The need here is to remove the harmful substances from the environment [6].

In the separation of heavy metal compounds from wastewater, methods such as ion exchange, adsorption and extraction can be listed. Inefficiency and economic application difficulties can be shown as the biggest problems encountered. The effectiveness of membrane filtration techniques, such as ultrafiltration and nanofiltra-

tion, in the removal of heavy metals has been investigated. Apart from this, in some studies, the efficiency of the adsorption method was explained by the use of adsorptive membranes. From extraction examples, solvent toxicity limits the application in industrial scale applications. The need for a large amount of solvent for heavy metal recovery is undesirable in terms of cost and toxicity. In addition to commercially used membrane separation and electrodialysis methods, there are also techniques used in full or pilot scale applications and emerging technologies such as selective adsorption [6–10].

Recently, polymer inclusive membranes (PIMs) based on the principle of ion exchange have become increasingly important due to their ease of application, cost, sustainability and many other prominent features. PIM has better mechanical properties and chemical resistance than backing liquid membranes. Adding plasticizers to the polymer membrane helps blend the carrier with the polymer matrix and results in increased membrane flexibility [11]. PIMs are thin, flexible and stable and consist of base polymer, carrier and plasticizer members. Plasticizers are used in the plasticization of the polymer matrix and as solvents for the carrier, while their chemical and mechanical properties improve membrane performance by providing stability and flexibility to the membrane. Carriers are responsible for the desired ion exchange process. The versatility and ease of application of PIMs in terms of the target chemical species to be transported is ideal for problem solving [12, 13]. Polymer inclusive membranes are obtained, in practice, by applying the components of a polymer (such as cellulose triacetate, CTA), a carrier and a plasticizer (such as 2-nitrophenyl octyl ether, NPOE) in a solvent (dichloromethane) [13].

The critical point when designing PIMs is the specificity of the carrier. Removing the target chemical material and/or materials in a controllable manner and at the desired efficiency level constitutes the solution. This will be understood as a result of optimization studies and investigation of membrane efficiency and sustainability. While ion carriers known in membrane studies provide effective separation, their low selectivity is seen as a disadvantage. For this reason, studies have been intensified for new compounds that are desired to provide selective separation from aqueous solutions [5]. In another study on the selective transport and removal of Cd from chloride solutions by polymer inclusion membranes, the selectivity of the transport process was investigated. In the study using Aliquat 336 as an ion carrier, Cd was effectively separated from chloride solutions [14].

The aim of this study was to determine the efficiency of the carrier used and its selectivity among target heavy metals. Accordingly, the study investigated the transport efficiency of synthesized pyridin-2-amine functionalized thiadiazol on polymer-containing membranes for Ni, Co, Cd, Cu and Pb heavy metals with high efficiency and target selectivity. For this purpose, 3-[5-(cycloheximino)-4,5-dihydro-1,3,4-thiadiazol-2-yl]pyridin-2-amine was synthesized and employed as an additive material in the presence of cellulose triacetate (CTA) and *o*-NPOE to prepare a novel pyrazole derivative embedded polymer inclusion membrane (Py@PIM). SEM, TGA and FT-IR techniques were carried out to determine the structure and surface morphology of Py@PIM. As a result of the study, Py@PIM synthesized using pyridin-2-amine functionalized thiadiazole was shown to be effective and selective in the transport of 5 heavy metals (Co, Cd, Cu, Ni, Pb) used in the study.

RESULTS AND DISCUSSION

Synthesis. 3-[5-(Cycloheximino)-4,5-dihydro-1,3,4-thiadiazol-2-yl]pyridin-2-amine was successfully synthesized by reacting 2-aminonicotinic acid with cyclohexylthiosemicarbazide as depicted in Scheme 1 [15, 16].

In the ATR-FTIR spectrum of 3-[5-(cycloheximino)-4,5-dihydro-1,3,4-thiadiazol-2-yl]pyridin-2-amine, the vibration band associated with the NH_2 group was recorded at 3282.1 cm^{-1}, while a band corresponding to NH stretching vibrations was observed at 3147.6 cm^{-1}. Bending vibrational bands appeared at 1442.7 cm^{-1}. Aromatic CH stretching vibrations in the pyridine ring were identified at 3045.0 cm^{-1}, and aliphatic CH stretching vibrations were recorded at 2922.9 and 2850.4 cm^{-1}. Sharp band at 1627.7 cm^{-1} was attributed to C=C bond stretching vibrations, and band at 690.2 cm^{-1} was assigned to C–S–C bond stretching vibrations. The C=N bond stretching vibrations were observed at 1557.8 cm^{-1}. The ^{1}H and ^{13}C NMR spectra are presented in Figs. S1 and S2 (see Supplementary Information). Signals corresponding to aliphatic protons were observed in the range of 1.26 to 3.67 ppm. Aromatic protons were detected between 6.63 and 7.97 ppm, the NH_2 proton peak appeared at 7.40 ppm, and the NH proton peak was found at 8.03 ppm. Additionally, the structure of 3-[5-(cycloheximino)-4,5-dihydro-1,3,4-thiadiazol-

Scheme 1.

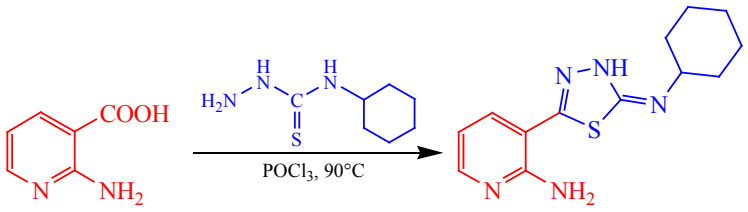

2-yl]pyridin-2-amine was further examined using two-dimensional COSY and HETCOR (HMBC) experiments (Figs S3 and S4, see Supplementary Information). The corresponding geminal protons were assigned based on the COSY correlations at 1.26, 1.57, 1.71, and 1.99 ppm (H^1, H^2, and H^3). Similarly, four geminal protons were assigned based on the COSY correlations at 1.26 (H^3) and 3.67 ppm (H^4). For the aromatic protons in the pyridine ring, a peak indicating a coupling interaction between H^7 at 6.63 ppm and H^6 at 7.97 ppm was observed. A similar interaction was noted between H^7 at 6.63 ppm and H^8 at 7.61 ppm. A four-bond HMBC correlation indicates a coupling between H^6 and the C^7, C^8 carbons. The data obtained were consistent with the literature [16].

Py@PIM was prepared using pyridin-2-amine functionalized thiadiazole, cellulose triacetate as polymer and 2-nitrophenyl octyl ether as plasticizer and ion carrier.

Characterization of Py@PIM. According to the TGA decomposition of the membrane prepared (Fig. 1), the thermal decomposition occurs in two stages. The first stage occurred around 250°C and it is thought that this decomposition is due to the ligand in the membrane. The decomposition at about 380°C, which occurs in the second stage, is the decomposition of cellulose triacetate and is also consistent with the literature [17].

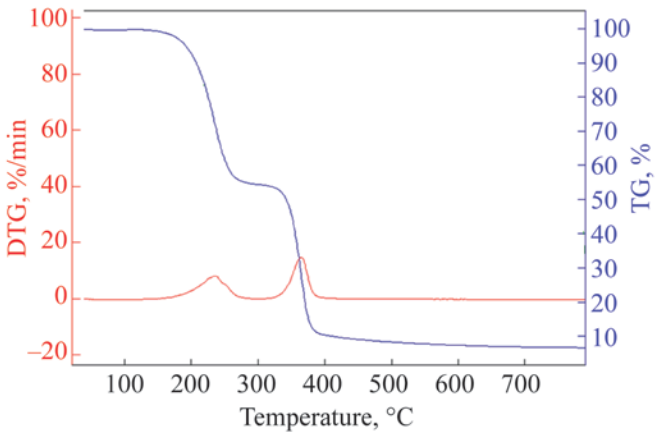

Fig. 1. The TGA curves of Py@PIM.

Figure 2 shows the SEM photographs of the surface morphology of the polymer inclusion membrane without calixarene and Py@PIM. As one can clearly see from Fig. 2, by the introduction of pyridin-2-amine functionalized thiadiazole, the polymer inclusion membrane surface became rougher with increased pore sized. This finding attributed that the substituted calixarene with mercapto functional groups make the polymer inclusion membrane to have nodular structure, with rough surface and increased pore size.

The IR spectrum of Py@PIM is given in Fig. S5 (see Supplementary Information) . In the spectrum, stretching vibrations of CH (2900 cm^{-1}) and C=O group (1740 cm^{-1}) were observed, while C–O backbone vibration was registered at 1020–1040 cm^{-1}. The NH stretching vibrations, aromatic and aliphatic CH stretching vibrations of the amine groups of the ligand were below the CTA stretching vibrations. Around 1600 cm^{-1}, the C=C and C=N stretching vibrations of the ligand were observed. The C–S–C stretching vibration of the ligand was recorded at around 690 cm^{-1}, the data are consistent with the literature [18].

Transport studies. The flux values of trace metals are calculated from the time profile and the receiving phase concentration of the initial phase technique and the results are given in Table 1. In single species experiments where each cation was placed individually in the dialysis cells, the kinetic coefficient of lead was higher than the other cation types. When compared with Ni, the kinetic coefficient of Pb was 2 times higher, while the difference was much higher when compared with Cd and Co. The prepared membrane did not pass Cu(II) ions. According to the kinetic coefficient, the order is Pb > Ni > Co > Cd > Cu. Similar kinetic order was also observed in multiple cation experiments, in experiments where all cations were mixed in a single cell. A similar ranking was observed in the flow (J_i) results. Pb showed the best flow in both single

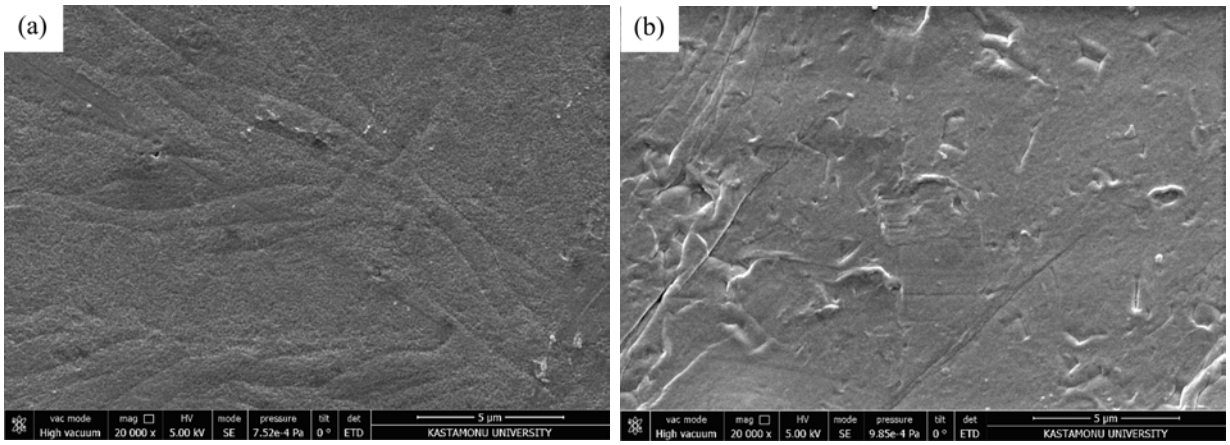

Fig. 2. The SEM images of membrane without pyridin-2-amine functionalized thiadiazole (a) and Py@PIM (b).

and competitive trials. This result is also proportional to the permeability coefficient data.

RF values for Pb^{2+} are higher than other metal ions for Pb^{2+} compared to other metal ions, but the corresponding ion sizes of Py@PIM are not significantly different (i.e. Pb^{2+} 78 pm, Cu^{2+} 73 pm, Ni^{2+} 69 pm, Cd^{2+} 95 pm and Co^{2+} 75 pm) show proximity correspond to similar electron densities. The most probable cause of this investigation is that Pb^{2+} can flow more easily to the hydration spheres to enter hydropological Py@PIM medium. This is reflected by the hydration energies of the abovementioned cations where Cu^{2+}, Ni^{2+}, Cd^{2+} and Co^{2+} are 2099, 2096, 1809 and 2010 kJ/mol, respectively.

Stability of Py@PIM. To assess the life of the Py@PIM, the carrying capacity of the membrane for Pb^{2+} was examined under the same experimental conditions (feed phase: 0.1 mol/L HCl solution: receptor phase: 10^{-4} mol/L Pb^{2+}). There were four repetitive membrane transport experiments using the same membrane for Pb^{2+}. This membrane was removed from the cell and washed in deionized water. The permeability coefficient of Pb^{2+} changed slightly after four cycles of 48 h each. Table 2 shows the variation of the observed Pb^{2+} flux throughout the four experiments. As can be seen, the membrane has good stability because the decrease in flux is very small. In addition, no structural deformation was observed in the membranes when the experiments were completed.

CONCLUSIONS

This study showed that inclusion of pyridin-2-amine functionalized thiadiazole in the PIM structure was achieved, and the obtained Py@PIM could be successfully used for the facilitated transport of Ni^{2+}, Pb^{2+}, Cu^{2+}, Cd^{2+} and Co^{2+} ions. Moreover, selectively transport of Pb^{2+} ions were achieved by prepared Py@PIM. The results also showed that the transport efficiency of Py@PIM

Table 1. Single and multiple transport experiments using Py@PIM

Parameter	Cd	Co	Pb	Ni	Cu
Single experiment					
K, S^{-1}	1.98E-5	7.49E-5	2.06E-4	1.04E-4	–
P, m/s	3.55E-5	3.58E-6	9.88E-6	4.97E-6	–
J_i, mol m^{-2} s^{-1}	1.34E-6	4.41E-5	3.69E-5	3.05E-5	–
RF	6.88	23.60	47.93	31.18	
Multiple experiment					
K, S^{-1}	1.98E-5	6.79E-5	1.69E-4	1.02E-4	–
P, m/s	9.48E-7	3.25E-6	8.06E-6	4.90E-6	–
J_i, mol m^{-2} s^{-1}	1.70E-6	4.83E-5	3.66E-5	3.27E-5	–
RF	6.88	21.68	45.49	30.82	

Table 2. Stability of Py@PIM (Pb^{2+})

Cycle number	J_i, mol m^{-2} s^{-1}
1	3.69E-5
2	3.12E-5
3	2.55E-5
4	2.51E-5

is repeatable and may be recommended for long-term separation. This result shows that the above-mentioned PIM-based separation approach has been promised for the development of efficient and environmentally friendly technologies for the cleaning of trace metals from contaminated waters.

EXPERIMENTAL

Cellulose triacetate (CTA-678.6 g/mol) was purchased from Sigma-Aldrich. Other chemicals like hydrochloric acid, dimethylformamide, dichloromethane, Pb, Ni, Co, Cd, Cu, and NaOH were purchased from Merck chemicals and Fluka. All solutions were prepared using ultra-pure water from a Milli-Q (Millipore Corp.).

A Gallenkamp instrument in a sealed capillary tube was used to define melting points. NMR spectra were recorded on a Bruker 400 MHz spectrometer. TLC silica gel plates (SiO_2, Merck PF254) were used for analytical thin-layer chromatography studies.

3-[5-(Cycloheximino)-4,5-dihydro-1,3,4-thiadiazol-2-yl]pyridin-2-amine was prepared as previously described [15, 16]. IR spectrum, ν, cm^{-1}: 3282.1 (NH_2), 3147.6 (NH), 1442.7 (NH), 3045.0 (CH_{Ar}), 2922.9, 2850.4 (CH_{Alk}), 1627.7 (C=C), 1557.8 (C=N), 690.2 (C–S–C). ^{1}H NMR spectrum (DMSO-d_6), δ, ppm: 1.26 m (5H, cyclohexyl CH_2), 1.57 m (1H, cyclohexyl CH_2), 1.71 m (2H, cyclohexyl CH_2), 1.99 m (2H, cyclohexyl CH_2), 3.67 s (1H, cyclohexyl CH), 6.63 t (1H, CH_{Py}), 7.40 br. s (2H, NH_2), 7.61 d (1H, CH_{Py}), 7.97 d (1H, CH_{Py}), 8.03 s (1H, thiadiazole NH). ^{13}C NMR spectrum (DMSO-d_6), δ_C, ppm: 166 (C^{11}), 157 (C^6), 155 (C^{10}), 149 (C^5), 138 (C^8), 113 (C^7), 108 (C^9), 54 (C^4), 33 (C^3), 25 (C^1), 24 (C^2). Found, %: C 56.78; H 6.10; N 25.48. $C_{13}H_{17}N_5S$. Calculated, %: C 56.71; H 6.21; N 25.41. The data obtained were found to be compatible with the literature [15, 16].

Polymer inclusion membrane preparation. For the membrane used in the studies, cellulose triacetate (CTA, 0.12 g) was used as polymer, 2-nitrophenyl octyl ether (2-NPOE) (0.15 mL) as plasticizer and ion carrier (10 mg). This mixture was prepared by dissolving in dichloromethane. The homogeneous mixture obtained was poured into a Petri dish with a diameter of 9 cm to evaporate the solvent. The membrane was then separated from the Petri dish and washed in deionized distilled water. A digital micrometer Mitutoyo was used to measure the thickness of the membrane by taking 10 readings with a precision of 0.1 micrometer. The same procedure was repeated without ion carrier for control experiments.

The thermal properties of the membrane were determined using a Seteram Instrumentation Labsys Evo (France). Membrane samples were weighed 10 mg, hermetically sealed in aluminium containers and heated at 10 deg/min between 0 and 800°C under a nitrogen atmosphere to prevent thermo-oxidative reactions.

Transport experiments. In order to realize the transport of trace amounts of metal ions in aqueous solution, a cell consisting of two separable sections made of Teflon was used [19]. The membrane was placed between two 46 mL cells, the donor cell and the acceptor cell, with the help of a clamp using a Teflon seal. The donor cell contained trace metal ions while the receiver cell contained deionized water. During the experiment, the magnetic stirrer rotated at a speed of 500 rpm in both cells and the flow was ensured with magnetic fish. Afterwards, 1 mL each was taken from the acceptor and donor cells at certain intervals and the measurement was made using ICP-OES for each. The surface area of the membrane in contact with aqueous solutions is 9.6 cm^2. The rate of metal transport can be considered to be proportional to the difference in concentrations in the donor and acceptor cell. In this case, the metal ion transfer coefficient (k, 1/s) in the donor cell can be calculated using the first order kinetic equation (1).

$$\ln\frac{c}{c_i} = -kt, \quad (1)$$

where c (mol/m^3) is concentration of metal ions in a time t; c_i (mol/m^3) is initial concentration of metal ions.

To analyze the studied process of transport of metal ions, the following values were taken into account. Initial stream J_i, mol m^{-2} s^{-1}:

$$J_i = \left(\frac{V}{A}\right)kc_i, \quad (2)$$

where V (m^3) is volume of feeding phase; A, m^2 is a membrane surface.

Permeability coefficient P, m/s:

$$P = \left(\frac{V}{A}\right)k. \quad (3)$$

Recovery factors of the trace metals (RF, %) were calculated from following equation:

$$\mathrm{RF} = \left(1 - \frac{c_r}{c_f}\right) \times 100, \quad (4)$$

where c_r and c_f (mol/L) are the metal concentrations in the receiver and feed phases, respectively.

Stability of PIM. The stability of Py@PIM was evaluated on the basis of the first flux values obtained from four sequential experiments in which the membrane was used under the experimental conditions (feeding phase: 0.1 mol/L HCl solution: receiving phase: 10^{-4} mol/L Pb^{2+}).

FUNDING

This work was supported by ongoing institutional funding. No additional grants to carry out or direct this particular research were obtained.

CONFLICT OF INTEREST

The authors declare no conflict of interest.

SUPPLEMENTARY INFORMATION

The online version contains supplementary material available at https://doi.org/10.1134/S1070363224080176.

REFERENCES

1. Sgarlata, C., Arena, G., Longo, E., Zhang, D.M., Yang, Y.F., and Bartsch, R.A., *J. Membrane Sci.,* 2008, vol. 323, no. 2, p. 444. https://doi.org/10.1016/j.memsci.2008.07.004
2. Sellami, F., Kebiche-Senhadji, O., Marais, S., Couvrat, N., and Fatyeyeva, K., *React. Funct. Polym.,* 2019, vol. 139, p. 120. https://doi.org/10.1016/j.reactfunctpolym.2019.03.014
3. Motsoane, N., Maiphetlho, K., Ncube, S., Richards, H., Kotze, I., Tutu, H., Cukrowska, E., and Chimuka, L., *Environ. Technol. Innov*., 2020, vol. 19, Article ID 100939. https://doi.org/10.1016/j.eti.2020.100939
4. Pospiech, B., *Arch. Metal Mater.,* 2015, vol. 60, no. 4, p. 2933. https://doi.org/10.1515/amm-2015-0468
5. Engin, M.S., Sayin, S., Cay, S., Kir, E., and Sardohan-Koseoglu, T., *Int. J. Environ. Anal. Chem.,* 2019, vol. 99, no. 11, p. 1103. https://doi.org/10.1080/03067319.2019.1616706
6. Zulkefeli, N.S.W., Weng, S.K., and Halim, N.S.A., *Curr. Pollut. Rep.*, 2018, vol. 4, no. 2, p. 84. https://doi.org/10.1007/s40726-018-0091-y
7. Khulbe, K.C. and Matsuura, T., *Appl. Water Sci.,* 2018, vol. 8, no. 1, Article ID 19. https://doi.org/10.1007/s13201-018-0661-6
8. Vo, T.S., Hossain, M.M., Jeong, H.M., and Kim, K., *Nano Converg.,* 2020, vol. 7, no. 1. Article ID 36. https://doi.org/10.1186/s40580-020-00245-4
9. Xiang, H.R., Min, X.B., Tang, C.J., Sillanpää, M., and Zhao, F.P., *J. Water Process Eng.*, 2022, vol. 49, Article ID 103023. https://doi.org/10.1016/j.jwpe.2022.103023
10. Benosmane, N., Hamdi, S.M., Hamdi, M., and Boutemeur, B., *Sep. Purif. Technol.*, 2009, vol. 65, no. 2, p. 21. https://doi.org/10.1016/j.seppur.2008.10.039
11. Nghiem, L.D., Mornane, P., Potter, I.D., Perera, J.M., Cattrall, R.W., and Kolev, S.D.. *J Membrane Sci.,* 2006, vol. 281, nos. 1–2, p. 7. https://doi.org/10.1016/j.memsci.2006.03.035
12. Keskin, B., Zeytuncu-Gökoglu, B., and Koyuncu, I., *Chemosphere,* 2021, vol. 279. Article ID 130604. https://doi.org/10.1016/j.chemosphere.2021.130604
13. Engin, M.S., Sayin, S., and Cay, S., *J. Incl. Phenom. Macro.,* 2018, vol. 92, nos. 1–2, p. 173. https://doi.org/10.1007/s10847-018-0831-z
14. Pont, N., Salvadó, V., and Fontàs, C., *J. Membrane Sci.,* 2008, vol. 318, nos. 1–2, p. 340. https://doi.org/10.1016/j.memsci.2008.02.057
15. Yakan, H., *Turk. J. Chem.,* 2020, vol. 44, no. 4, p. 1085. https://doi.org/10.3906/kim-2002-76
16. Sener, N. and Aldwib, A.E.O., *Chem. Biodivers.,* 2024, vol. 21, Article ID e202400. https://doi.org/ 10.1002/cbdv.202400522
17. Nouh, S.A., Wahab, L.A., and Eissa, H.M., *Radiat. Meas.,* 1999, vol. 30, no. 6, p. 753. https://doi.org/10.1016/S1350-4487(99)00234-6
18. Fan, X.S., Liu, Z.T., and Liu, Z.W., *J. Hazard. Mater.,* 2010, vol 177, no. 1–3, p. 452. https://doi.org/10.1016/j.jhazmat.2009.12.054
19. Koseoglu, T.S., Kir, E., Ozkorucuklu, S.P., and Karamizrak, E., *React. Funct. Polym.,* 2010, vol 70, no. 11, p. 900. https://doi.org/10.1016/j.reactfunctpolym.2010.08.004